Inventory of Supplemental Information: Liu, Tose et al.

Supplementary Figures and Legends:

Supplementary Figure Legends

Figure S1. Fiber photometry of VTA DA cell bodies, Related to Figure 2.

(A) Histological verification (left) and sample fluorescent image (right) of GCaMP6m (green) expression and optical fiber placements in VTA of DAT-Cre mice (n = 11 mice) used for experiments shown in **Figures 2A-2E** (red - tyrosine hydroxylase (TH), blue – DAPI; IPN: interpeduncular nucleus, VTA: ventral tegmental area, SN: substantia nigra, ml: medial lemniscus, DAT: dopamine transporter) (scale bar 200 μm).

(B) Animals were randomly divided into two groups and the initial nicotine dose was counter-balanced across days.

(C) No significant (ns) difference in VTA DA GCaMP6m activity between sub-group 1 (turquoise, n = 5 mice) or sub-group 2 (purple, n = 6 mice) in response to rewarding (left) or aversive (right) nicotine (area of light shading represents SEM).

(D) AUCs of averaged VTA DA GCaMP6m response to saline (grey), rewarding nicotine (blue), and aversive nicotine (red) (within-animal, n = 11 mice) of equivalent time bins (15 s) demonstrates a significantly different response across time only in the aversive nicotine condition (*** $p < 0.001$; data represent means ± SEM).

(E) Left: Averaged VTA DA GCaMP6m responses for individual infusions during the early component (0-15s) reveal consistent activation of VTA DA cells by rewarding nicotine, but a gradual suppression of activity by aversive nicotine after the first infusion. Right: The inhibitory effects of aversive nicotine are less pronounced during the remainder of the 60s post-infusion response and the activation by rewarding nicotine gradually decreases with each infusion (gap denotes separate analyses for infusion 1 and infusions 2-6 due to non-normal distribution, * $p < 0.05$, ** $p < 0.01$, *** $p < 0.001$; data represent means ± SEM).

(F) Sample whole traces from a representative animal receiving saline (grey), rewarding nicotine (blue) or aversive nicotine (red).

(G) Histological verification (left) and sample fluorescent image (right) of GCaMP6m expression and optical fiber placements in VTA of DAT-Cre mice (n = 11 mice) used in experiments shown in **Figures 2H-2K** (scale bar 200 μm).

Figure S2. Fiber photometry recordings of dLight and GCaMP in separate NAc subregions, Related to Figure 3.

(A) Left: Histological verification of dLight1.2 expression and optical fiber placements in NAc medial shell (NAcMed) and NAc lateral shell (NAcLat) for experiments shown in **Figures 3A-3F**. Middle: Sample fluorescent images of the respective brain structures (green – dLight1.2; scale bars 200 μm). Right: To facilitate within-animal comparisons of nicotine dose, the order of nicotine dose was counterbalanced between two randomly assigned sub-groups.

(B) Averaged whole traces of dLight response to the rewarding dose of nicotine in NAcMed and NAcLat (area of light shading represents SEM).

(C) Peri-infusion plots of dLight fluorescence averaged across infusions for NAcMed (indigo) compared to NAcLat (turquoise). A 2-way ANOVA with multiple comparisons test for each time point from 1 s pre-infusion to 60 s post-infusion (10 Hz sample rate, n = 611 data points) revealed no significant (ns) differences between NAc subregions (area of light shading represents SEM).

(D) No order effect was observed between animals that received the aversive dose first (sub-group 1, pink) or the rewarding dose first (sub-group 2, green) in the NAcMed or NAcLat when performing a 2-way ANOVA with multiple comparisons test for each time point (n = 611 data points; area of light shading represents SEM).

(E) AUCs for dLight response to individual infusions of aversive nicotine (Av Nic, red) or saline (Sal, grey) in the NAcMed reveal that the increase of DA release during the early and late components occur primarily in response to the first infusion (gap denotes separate analyses for infusion 1 and infusions 2-6 due to non-normal distribution, ** $p < 0.01$, data represent means ± SEM).

(F) AUCs for dLight response to individual infusions during the early (left) and late (right) component in NAcLat (gap denotes separate analyses for infusion 1 and infusions 2-6 due to non-normal distribution, * $p < 0.05$, *** $p < 0.001$, data represent means ± SEM).

(G) Top left: Schematic of experimental design of targeting GCaMP6m to VTA DA neurons in DAT-Cre mice and implantation of optical fibers in NAcMed and NAcLat. Fiber photometry (FIP) recordings are performed during IV infusions of aversive nicotine. Top right: Histological verification of GCaMP6m expression in VTA and optical fiber placements in NAcMed and NAcLat. Bottom: Sample fluorescent images of GCaMP6m (green) expression in VTA (red –

TH, blue – DAPI; scale bar 200 μm) (left) and optical fiber placements in NAcMed and NAcLat (right) (scale bars 200 μm). No significant differences between dLight and GCaMP signals in either NAcMed or NAcLat when performing a 2-way ANOVA with multiple comparisons test for each time point (n = 611 points; area of light shading represents SEM).

(H) Top: Schematic of experimental design. Bottom: Sample fluorescent image and schematics showing histological verification of eYFP or eNpHR (green) expression in the VTA of DAT-Cre mice (red - TH); blue - DAPI) as well as verification of optical fiber locations in the NAcLat (scale bars 500 μm).

(I) Left: Schematic of real-time place preference/aversion assay. Animals received 589 nm light on different sides of the chamber. Right: Bar graph showing that eNpHR mice (n = 10) spent significantly less time in the light-paired side of the chamber compared to eYFP control mice (n = 6 mice) (* $p < 0.05$, data represent means ± SEM).

(J) Bar graph showing no significant differences in general locomotor behavior (with or without 589 nm light) in the open field test between eNpHR (n = 10 mice) and eYFP (n = 6 mice) mice.

(K) Left: Histological verification of dLight1.2 expression and optical fiber placements in NAcMed and NAcLat for experiments shown in **Figures 3G-3N**. Right: Sample fluorescent images of the respective brain structures (green – dLight, blue – DAPI) (scale bars 200 μm).

(L) AUCs of dLight response to individual infusions of aversive nicotine with pretreatment and co-infusion of antagonists in NAcMed during the early and late component (gap denotes separate analyses for infusion 1 and infusions 2-6 due to non-normal distribution, * $p < 0.5$, ** $p < 0.01$, *** $p < 0.001$; data represent means ± SEM).

(M) Same as in (L) but for NAcLat (gap denotes separate analyses for infusion 1 and infusions 2-6 due to non-normal distribution, * $p < 0.5$, ** $p < 0.01$, data represent means ± SEM).

Figure S3. VTA GABA response to rewarding or aversive nicotine, Related to Figure 4.

(A) Left: Histological verification of GCaMP6m expression and optical fiber placements in VTA of GAD2-Cre mice (n = 7 mice) for experiments shown in **Figures 4G-4J**. Right: Sample fluorescent image of the VTA showing TH-immunohistochemistry (red) and GCaMP6m (green) expression. Note, that TH-immunopositive cells do not co-express GCaMP6m (blue – DAPI, scale bar 200 μm).

(B) Averaged whole traces for saline (Sal, grey), rewarding nicotine (Rew, blue), and aversive nicotine (Av, red) infusions recorded in VTA GABA neurons. Inset: Comparison between first and last infusions (area of light shading represents SEM).
(C) AUCs for GCaMP response in VTA GABA neurons to individual infusions during the early (left) and late (right) components (gap denotes separate analyses for infusion 1 and infusions 2-6 due to non-normal distribution; EC: early component; LC: late component; * $p < 0.5$, ** $p < 0.01$, *** $p < 0.001$; data represent means ± SEM).
(D) Peri-infusion plot of averaged GCaMP response in VTA GABA neurons across infusions for saline (black), rewarding nicotine (blue), and aversive nicotine (red) (area of light shading represents SEM). Dots above traces denote significant differences from a multiple comparisons test after 2-way ANOVA (purple – rewarding versus aversive nicotine, blue – rewarding nicotine versus saline, red – aversive nicotine versus saline; * $p < 0.05$).
(E) AUCs for the early (left) and late (right) components averaged across infusions recorded in VTA GABA neurons. The aversive dose of nicotine elicits a significantly higher response compared to rewarding nicotine and saline conditions during the early component (*** $p < 0.001$, data represent means ± SEM).
(F) AUCs of GCaMP response in VTA GABA neurons to individual infusions of aversive nicotine with pretreatment and co-infusion of antagonists during the early (left) and late (right) components (gap denotes separate analyses for infusion 1 and infusions 2-6 due to non-normal distribution, * $p < 0.5$, *** $p < 0.001$; data represent means ± SEM).
(G) Averaged AUC GCaMP response in VTA GABA neurons to aversive nicotine with antagonists during the late component. Only MEC significantly reduced GCaMP activity in VTA GABA neurons in response to aversive nicotine (* $p < 0.05$, data represent means ± SEM).

Figure S4. Anatomy and connectivity of LDT GABA and glutamate neurons, Related to Figure 4.

(A) Left: VGLUT2-Cre (n = 3 mice) or GAD2-Cre (n = 3 mice) mice were injected with AAV-DIO-eYFP into the LDT to label glutamatergic (i.e., VGLUT2-expressing) or GABAergic (i.e., GAD2-expressing) cells, respectively. Middle: *in situ* hybridization was performed for *GAD1* and *GAD2* mRNA in VGLUT2-Cre animals and *VGLUT2* mRNA in GAD2-Cre animals to quantify co-expression of these genes. Only 4% of eYFP-positive cells in the LDT of VGLUT2-

Cre animals were also positive for *GAD1/GAD2* mRNA (n = 29/718 cells). Similarly, only 5% of eYFP-positive cells in the LDT of GAD2-Cre animals were also positive for *VGLUT2* mRNA (n = 52/987 cells). Right: Sample images showing eYFP-positive (green) cells in the LDT and express of *GAD1/GAD2* (top) or *VGLUT2* (bottom) mRNA. Yellow arrows indicate cells co-expressing *GAD1/GAD2* or *VGLUT2* mRNA and eYFP, whereas white arrows indicate cells that express eYFP but lack expression *GAD1/GAD2* or *VGLUT2* (scales bars 250 µm (left), 20 µm (right)).

(B) Left: VGLUT2-Cre (n = 4 mice) or GAD2-Cre (n = 3 mice) mice were injected with AAV-DIO-eYFP into the LDT. In the same animals, red fluorescent retrobeads were injected into the VTA to retrogradely label VTA-projecting LDT neurons. Middle: Co-labeling of beads-containing and eYFP-expressing LDT cells was quantified. In VGLUT2-Cre mice, 62% of beads-containing (i.e., VTA-projecting) LDT cells were also positive for eYFP (n = 323/525 cells). In GAD2-Cre mice, 30% of beads-containing (i.e., VTA-projecting) LDT cells were also positive of eYFP (n = 77/259 cells). Right: Sample images showing beads-labeled cells and eYFP-positive cells in the LDT of VGLUT2-Cre (top) and GAD2-Cre (bottom) mice. White arrows indicate eYFP-positive cells that contain retrobeads (scales bars 125 µm (left), 50 µm (right)).

(C) Left: VGLUT2-Cre (n = 8 mice) or GAD2-Cre (n = 5 mice) were injected with AAV-DIO-eYFP into the LDT and distribution of eYFP-positive terminals in the VTA and adjacent structures was analyzed. Right: Sample images demonstrating the qualitative difference between the distribution of eYFP-positive (green) terminals in the VTA from VGLUT2-Cre and GAD2-Cre animals (red – TH, blue - DAPI) (scales bars 250 µm (left), 125 µm (right)).

(D) Left: GAD2-Cre (n = 10 mice) were injected with AAV-DIO-synaptophysin-eYFP into the LDT and distribution of eYFP-positive terminals in the VTA was analyzed. Right: Sample fluorescent images showing synaptophysin-labeled (green) terminals in the VTA and IPN (blue – DAPI) (scales bars 250 µm (left), 125 µm (right)).

(E) Left: VGLUT2-Cre (n = 4 mice) and GAD2-Cre (n = 3 mice) mice were injected with AAV-flex-TVA-mCherry and AAV-flex-RG in the LDT to enable cell-type specific tracing of input neurons. Subsequent injection of RV-EnvA-ΔG-GFP into the VTA of the same VGLUT2-Cre and GAD2-Cre mice resulted in GFP-expression in cells that make direct monosynaptic input onto VTA-projecting $LDT_{Glutamate}$ or VTA-projecting LDT_{GABA} neurons, respectively. Right:

Schematic showing experimental design for mapping whole-brain inputs to VTA-projecting LDT_{GABA} neurons in a GAD2-Cre animal.

(F) Sample confocal images showing starter cells (mCherry-positive (red) and GFP-positive (green); yellow arrows), TVA-expressing (mCherry-positive, GFP-negative), and secondary/input cells (mCherry-negative, GFP-positive; white arrows) in the LDT of VGLUT2-Cre (top) and GAD2-Cre (bottom) mice (blue – DAPI) (scales bars 250 μm (left), 20 μm (right)).

(G) Bar graph showing quantification of starter cells, TVA-expressing and secondary cells in the LDT of GAD2-Cre (blue) and VGLUT2-Cre (red) mice (* $p < 0.05$, data represent means ± SEM).

(H) Horizontal and sagittal views of processed whole brains displaying brain-wide inputs to VTA-projecting $LDT_{Glutamate}$ (top) or VTA-projecting LDT_{GABA} neurons (bottom). Color code indicates different brain structures.

(I) Quantification of inputs to VTA-projecting LDT_{GABA} neurons (blue) and VTA-projecting $LDT_{Glutamate}$ (red) neurons. Data are presented as proportion of inputs counted in each individual brain structure. Color code corresponds to brain structures shown in (H) (Abbreviations: PFC – prefrontal cortex; green, Ctx – cortex; yellow, NAc – nucleus accumbens; blue, BNST – bed nucleus of the stria terminalis; magenta, VP – ventral pallidum; cyan, Amy – amygdala; yellow, Hab – habenula; white, LH – lateral hypothalamus; purple, PVH – paraventricular hypothalamus; red, Oth Hypo – other hypothalamic regions; green, ZI – zona incerta; white, MM – medial mammillary nuclei; purple, VTA – ventral tegmental area; yellow, SN – substantia nigra; magenta, IPN – interpeduncular nucleus; cyan, SupCxs – superior colliculus; blue, RMTg – rostromedial tegmental nucleus; green, PAG – periaqueductal gray; yellow, PnO – pontine nucleus oralis; magenta, DpMe – deep mesencephalic nucleus, cyan; DR – dorsal raphe; cyan, Oth raphe – other raphe nuclei; purple, PPT – pedunculopontine tegmentum; green, LDT – laterodorsal tegmentum; red, PB – parabrachial nucleus; blue, LC – locus coeruleus, magenta) (* $p < 0.05$, ** $p < 0.01$, *** $p < 0.001$; data represent means ± SEM).

(J) Sample image of fluorescent *in situ* hybridization in the LDT targeting mRNA for GAD2 (green) and α7 (white) (scale bar 10 μm).

(K) Bar graph showing significant larger number of LDT cells co-express α7 and GAD2 mRNA compared to LDT cells expressing α7 but lacking GAD2 mRNA (n = 3 mice; *** $p < 0.001$, data represent means ± SEM).

Figure S5. Fiber photometry of LDT_{GABA}→VTA neurons, Related to Figure 4.

(A) Left: Schematic showing experimental design for injection of GAD2-Cre animals (n = 6 mice) with AAV-DIO-GCaMP6m into the LDT and an optical fiber implanted in the VTA. During fiber photometry recordings, mice received IV infusions of saline, rewarding nicotine or aversive nicotine. Middle: Sample fluorescent images showing GCaMP (green) expression in the LDT (top, scale bar 200 μm) and optical fiber placement in the VTA (bottom, scale bar 200 μm) (red – TH, blue - DAPI). Right: Histological verification of GCaMP expression in LDT (top) and optical fiber placements in the VTA (bottom) (DTg - dorsal tegmental nucleus).

(B) Averaged whole traces of LDT_{GABA}→VTA GCaMP activity in response to saline (Sal, grey), rewarding nicotine (Rew, blue), and aversive nicotine (Av, red). Inset: Comparison between first and last infusion (area of light shading represents SEM).

(C) AUCs of GCaMP response in the LDT_{GABA}→VTA pathway to saline, rewarding nicotine, and aversive nicotine during the early (left) and late (right) components (gap denotes separate analyses for infusion 1 and infusions 2-6 due to non-normal distribution, * $p < 0.5$, data represent means ± SEM).

(D) Peri-infusion plot of averaged GCaMP response in the LDT_{GABA}→VTA pathway to saline (black), rewarding nicotine (blue), and aversive nicotine (red) (area of light shading represents SEM). Dots above traces denote time points where significant differences between conditions were observed from a multiple comparisons test following a 2-way ANOVA analysis (red – aversive nicotine versus saline, blue – rewarding nicotine versus saline, purple – rewarding nicotine versus aversive nicotine).

(E) Averaged AUCs of GCaMP signals in the LDT_{GABA}→VTA pathway across infusions during the early (left) and late (right) components (** $p < 0.01$; data represent means ± SEM).

(F) Left: Histological verification of GAD2-Cre animals (n = 7 mice) showing GCaMP expression and optical fiber placements in the VTA for experiments shown in **Figures 4K-4N**. Right: Sample fluorescent image of the VTA (green – GcaMP, red – TH, blue – DAPI; scale bar 200 μm).

(G) AUCs of GCaMP signals in the LDT_{GABA}→VTA pathway for individual infusions during the early component in response to IV administration of aversive nicotine (Av Nic) and antagonists (gap denotes separate analyses for infusion 1 and infusions 2-6 due to non-normal distribution, ** $p < 0.01$, data represent means ± SEM).

(H) AUCs of GCaMP signals in the LDT_{GABA}→VTA pathway for response to aversive nicotine and antagonists during the late component averaged across infusions (left) and for each infusion (right) (gap denotes separate analyses for infusion 1 and infusions 2-6 due to non-normal distribution; * $p < 0.05$, ** $p < 0.01$, *** $p < 0.001$; data represent means ± SEM).

Figure S6. Histological verification of caspase ablation, fiber photometry of NAc subregions and optogenetic inhibition of LDT_{GABA}→VTA pathway, Related to Figure 6.

(A) Histological verification of viral expression and optical fiber placements of GAD2-Cre animals (n = 6 mice) that were bilaterally injected with AAV-flex-TaCasp3 and AAV-DIO-mCherry into the LDT as well as dLight1.2 (green) into the NAcMed and NAcLat. The absence of mCherry-positive (red) cells in the LDT indicates successful ablation of LDT_{GABA} neurons (blue – DAPI; scale bars 200 μm (top) and 500 μm (bottom)).

(B) Histological verification of viral expression and optical fiber placements of GAD2-Cre control animals (n = 5 mice) that were injected bilaterally with AAV-DIO-mCherry into the LDT. dLight1.2 was infused into the NAcMed and NAcLat. Note the presence of mCherry-positive (red) cells in the LDT (blue – DAPI; scale bars 200 μm (top) and 500 μm (bottom)).

(C) Left: dLight1.2 AUCs during the early component for mCherry and Caspase groups in response to saline and aversive nicotine. Right: Same, but for the late component (gap denotes separate analyses for infusion 1 and infusions 2-6 due to non-normal distribution, * $p < 0.05$, ** $p < 0.01$, *** $p < 0.001$, data represent means ± SEM).

(D) Same as in (C) but for dLight1.2 recordings in NAcMed (gap denotes separate analyses for infusion 1 and infusions 2-6 due to non-normal distribution, * $p < 0.05$, ** $p < 0.01$, *** $p < 0.001$, data represent means ± SEM).

(E) Schematics showing histological verification of eNpHR and eYFP expression (green) in the LDT (top) and VTA (bottom). Grey dots indicate location of the optical fibers above the VTA.

(F) Bar graph showing no significant difference in time spent in the light-paired chamber between eNpHR mice (n = 5 mice) and eYFP mice (n = 4 mice) during the real-time place preference/aversion task (data represent means ± SEM).

(G) Bar graph showing no significant difference in general locomotor behavior between eNpHR (n = 4 mice) and eYFP (n = 4 mice) mice in the open field test with or without 589 nm light delivery (data represent means ± SEM).

Fig. S1 Liu, Tose et al.

Fiber photometry of VTA DA neurons

A

Histological verification

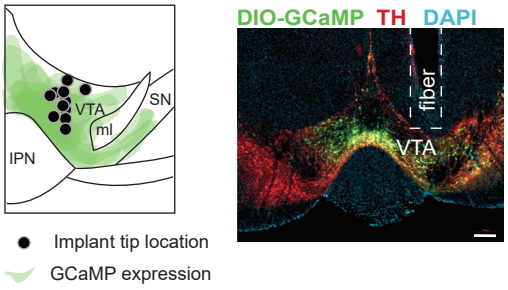

B

Counterbalanced nicotine doses

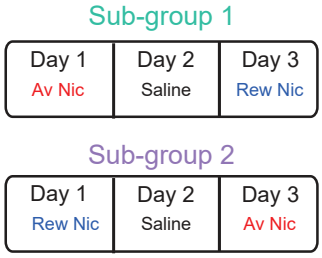

C

No order effect of nicotine doses

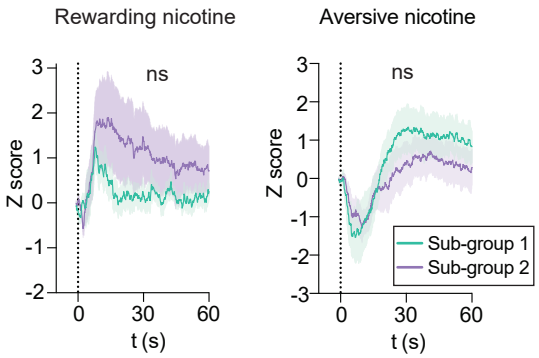

D

Biphasic response to aversive nicotine

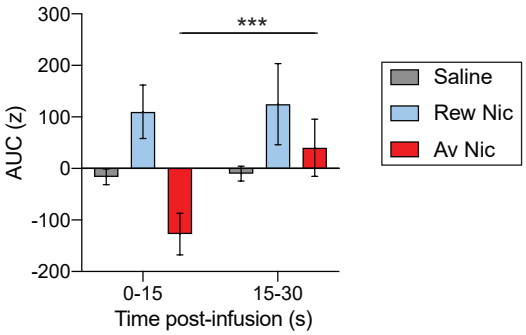

E

Response to individual infusions of nicotine

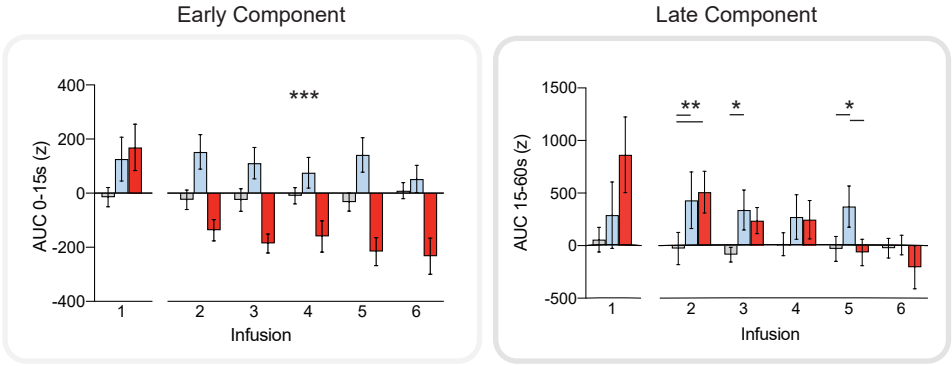

F

Sample traces from individual animal

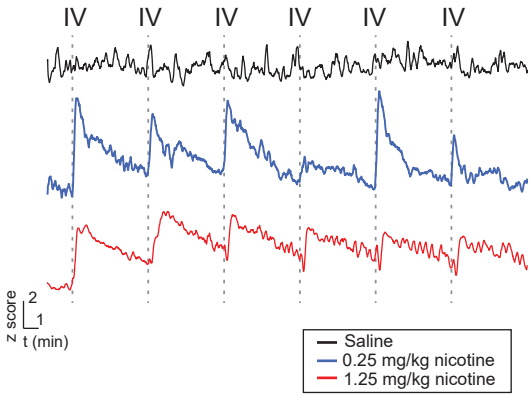

G

Fiber photometry of VTA DA neurons with DHBE

Histological verification

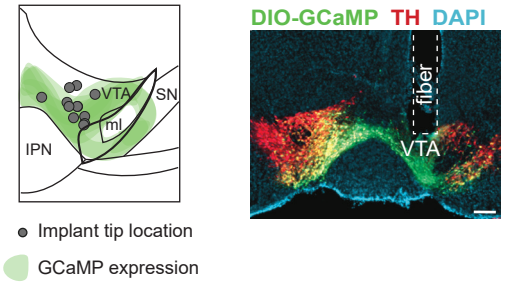

Fig. S2 Liu, Tose et al.

Fiber photometry recordings of dLight in NAc subregions

A

Histology

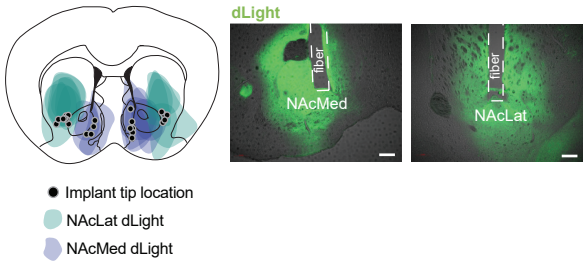

Counterbalanced doses

Sub-group 1		
Day 1	Day 2	Day 3
Av Nic	Saline	Rew Nic

Sub-group 2		
Day 1	Day 2	Day 3
Rew Nic	Saline	Av Nic

B

Averaged response to rewarding nicotine

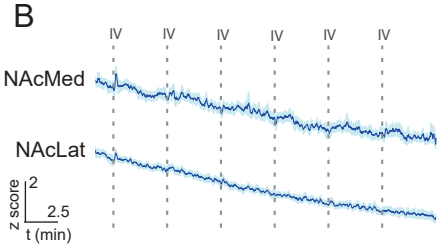

C

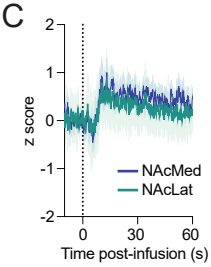

D

No order effect on aversive nic response

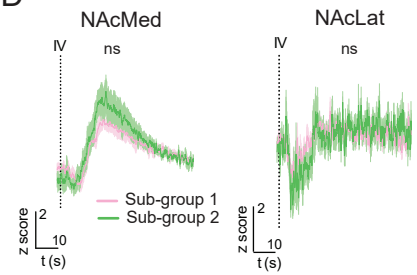

NAcMed

E

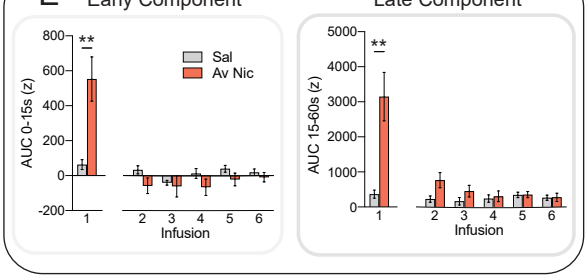

NAcLat

F

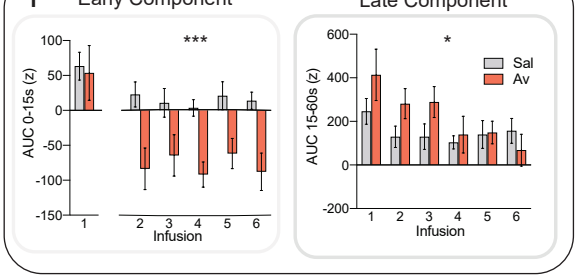

Terminal GCaMP is similar to dLight

G

Targeting DA axons in NAc

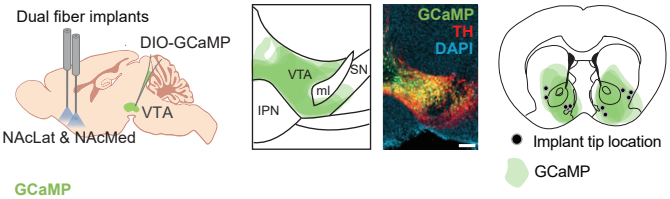

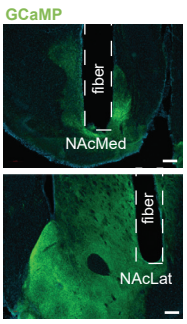

Averaged response to aversive nicotine

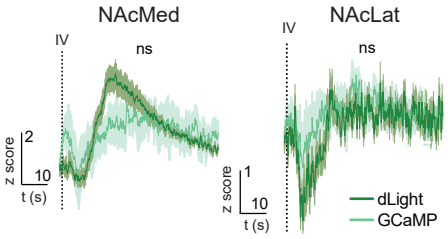

NAc dLight FIP with antagonists

K

Histological verification

L

NAcMed

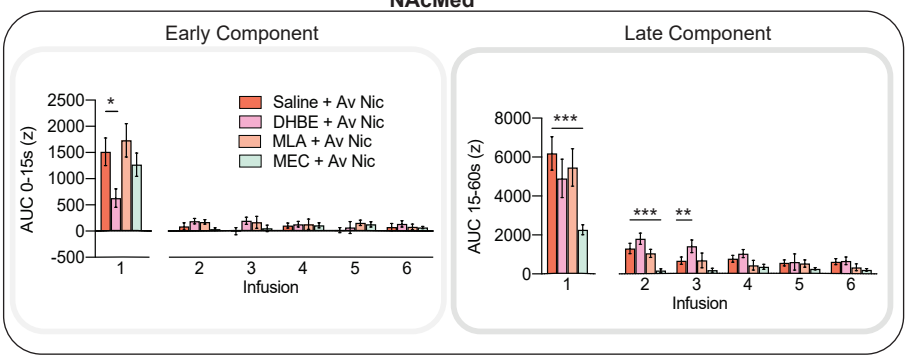

Optogenetic inhibition of VTA_{DA}→NAcLat

H

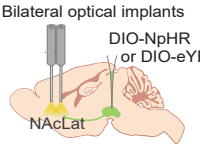

I

Real-time place aversion

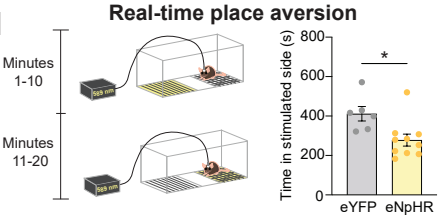

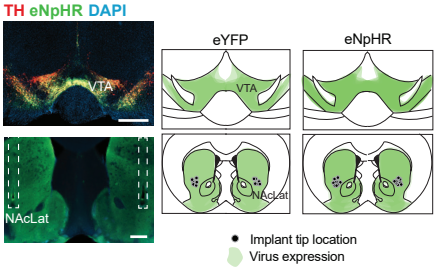

J

Open field test

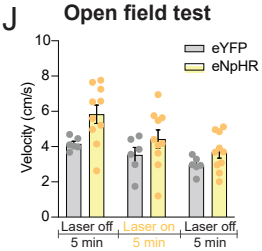

M

NAcLat

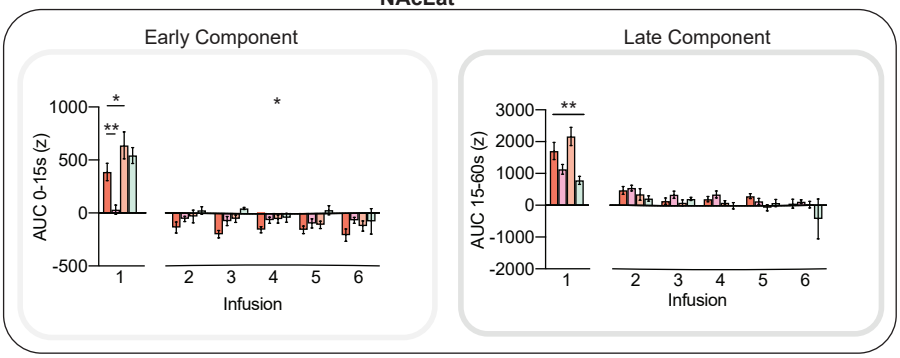

Fig. S3 Liu, Tose et al.

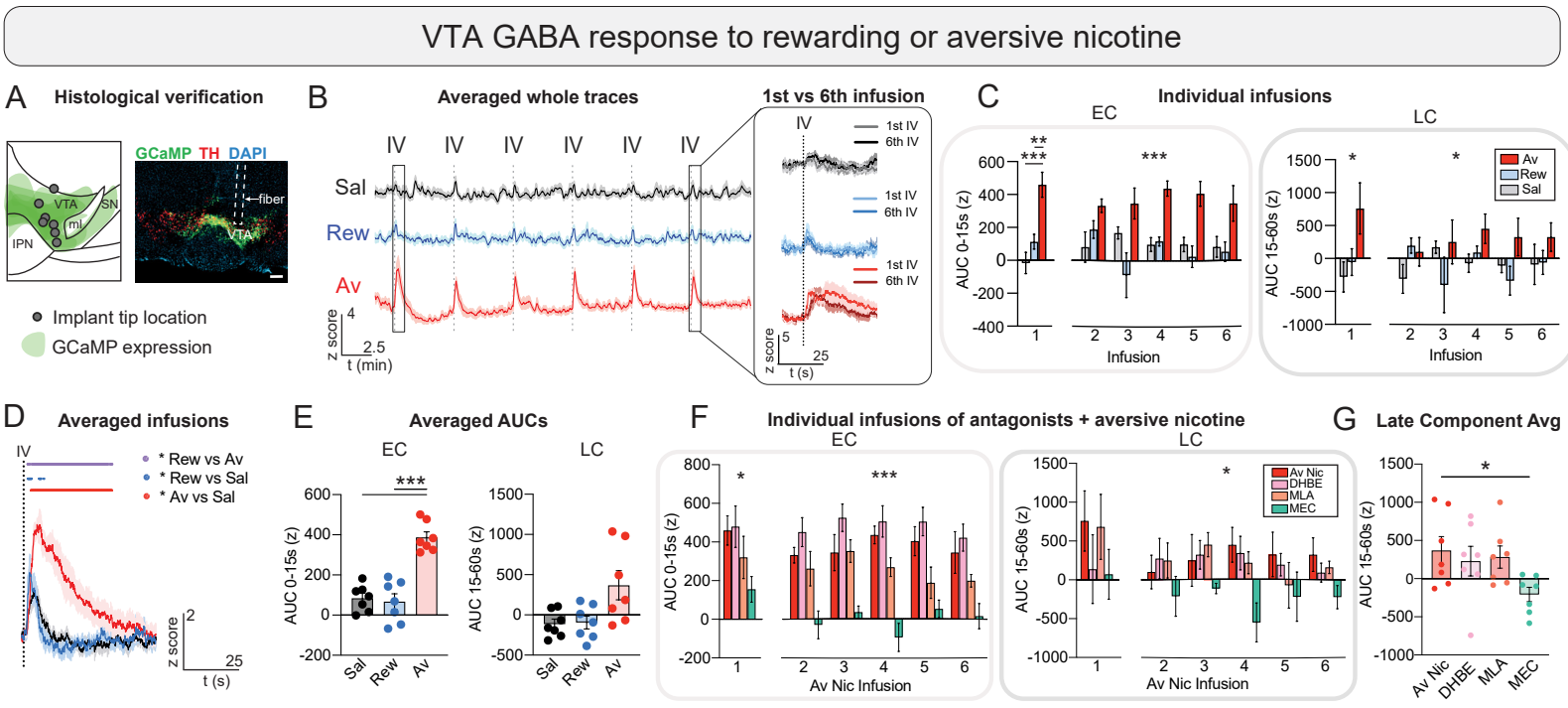

Fig. S4 Liu, Tose et al.

Anatomy and connectivity of LDT GABA and glutamate neurons projecting to VTA

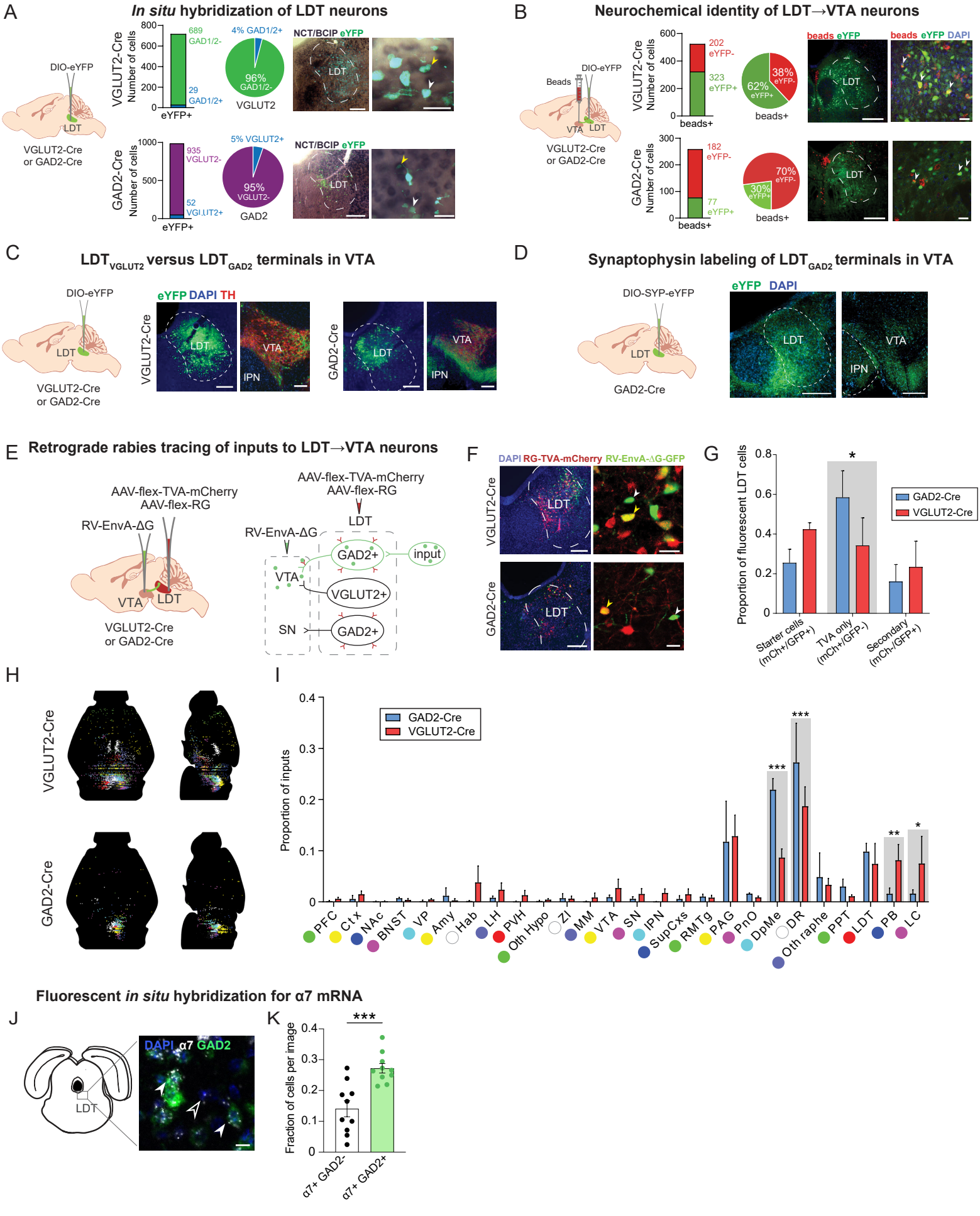

Fig. S5 Liu, Tose et al.

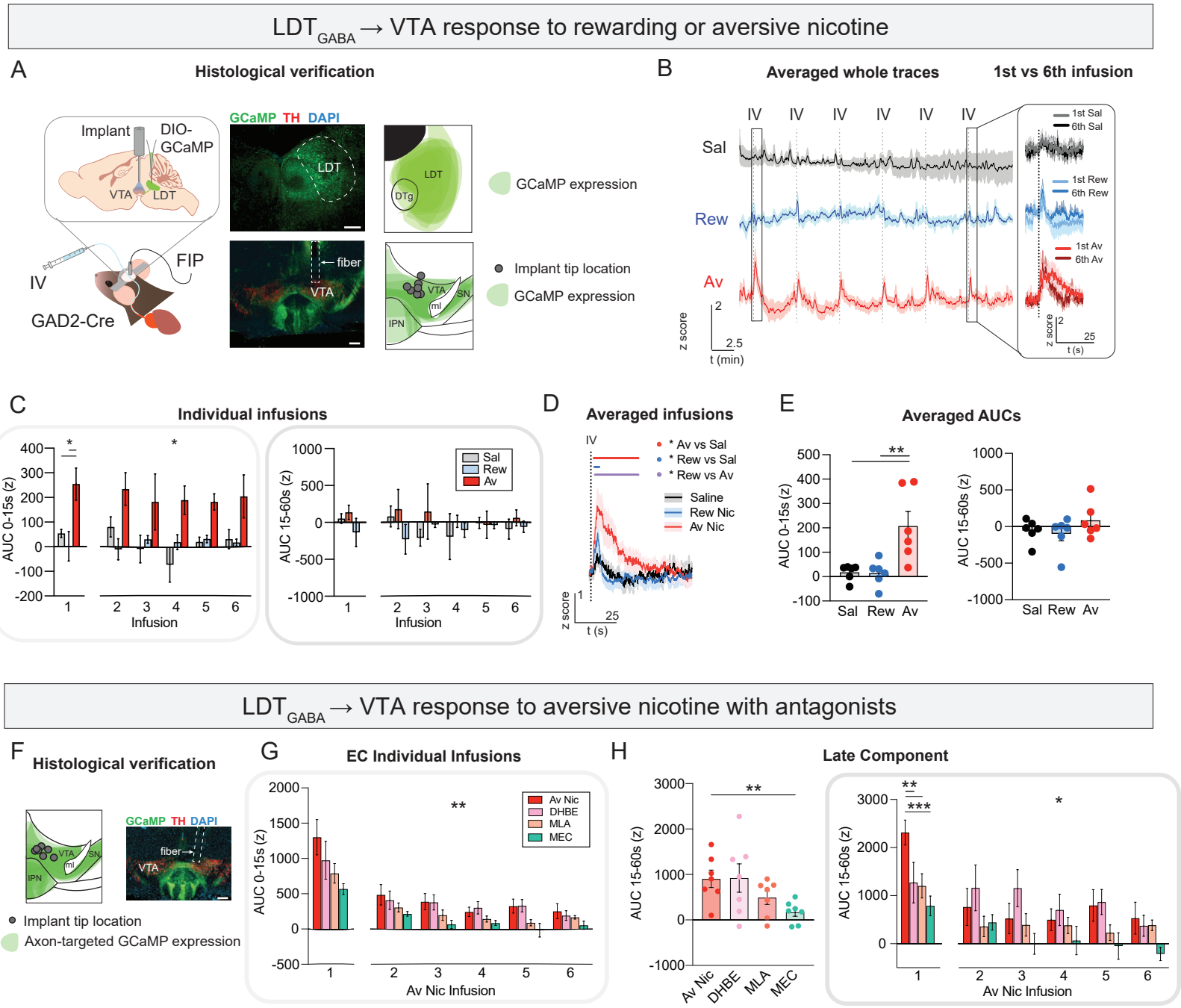

Fig. S6 Liu, Tose et al.

Histological verification of caspase ablation and fiber photometry of NAc subregions

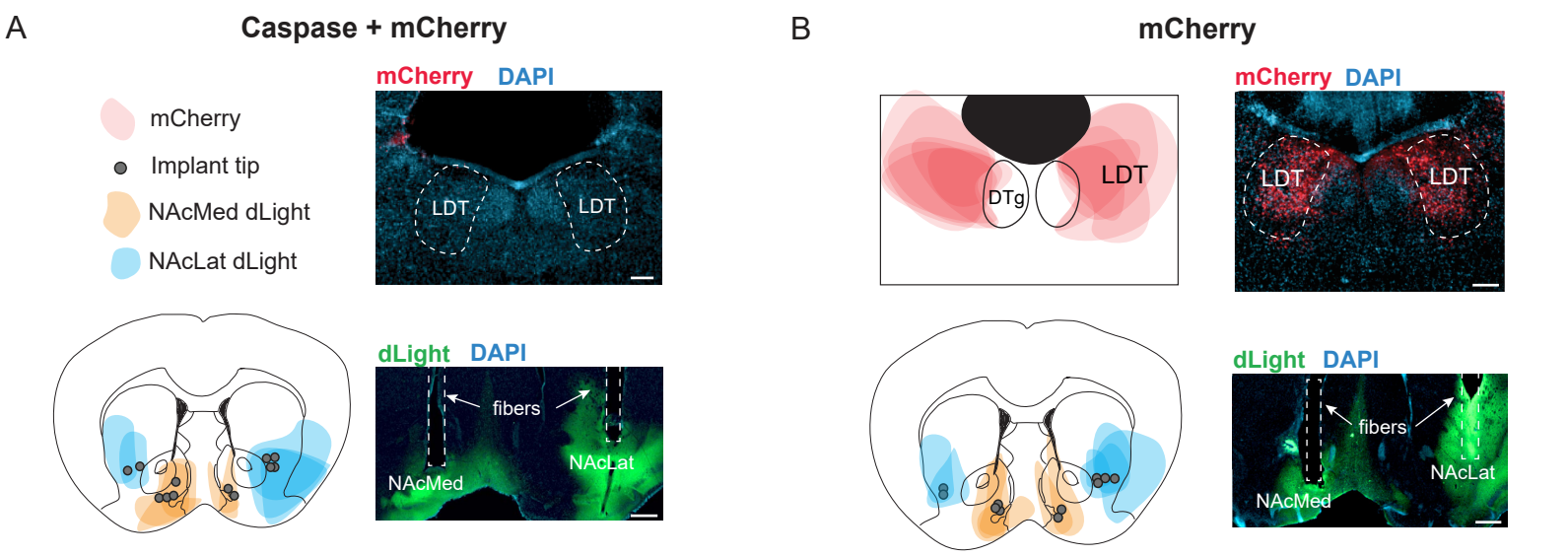

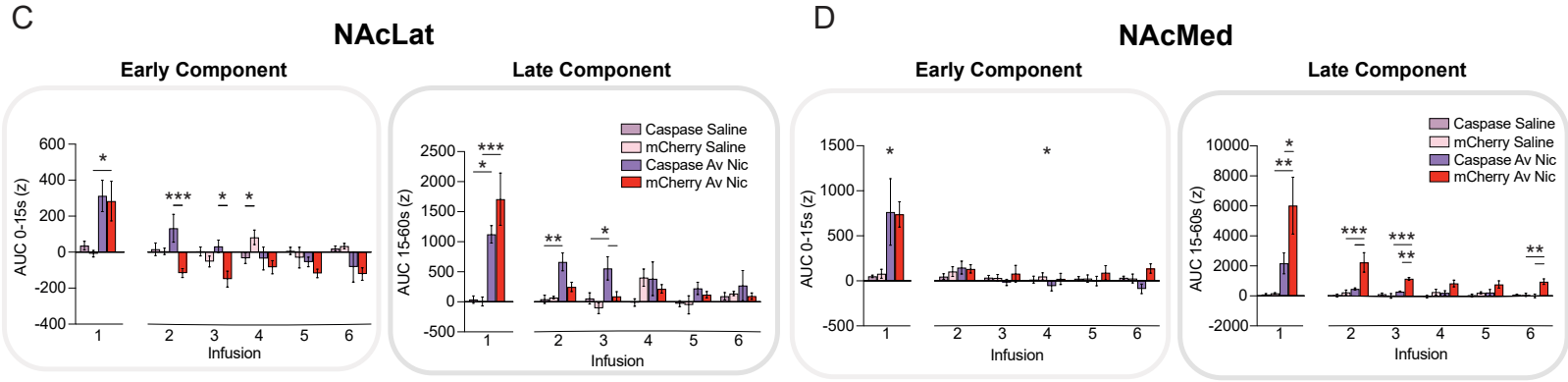

Optogenetic inhibition of LDT_{GABA} terminals in VTA does not alter behavior in absence of aversive nicotine